

---

# **Experiment and Numerical Simulation of Unsteady Temperature Fields in Automotive Catalytic Converters**

**Jian-Xin Wang, Shi-Jin Shuai and Ren-Jun Zhuang**  
State Key Lab. of Automotive Safety and Energy, Tsinghua Univ.

Reprinted From: Experimental Investigation of SI Engines  
(SP-1638)

The appearance of this ISSN code at the bottom of this page indicates SAE's consent that copies of the paper may be made for personal or internal use of specific clients. This consent is given on the condition, however, that the copier pay a per article copy fee through the Copyright Clearance Center, Inc. Operations Center, 222 Rosewood Drive, Danvers, MA 01923 for copying beyond that permitted by Sections 107 or 108 of the U.S. Copyright Law. This consent does not extend to other kinds of copying such as copying for general distribution, for advertising or promotional purposes, for creating new collective works, or for resale.

Quantity reprint rates can be obtained from the Customer Sales and Satisfaction Department.

To request permission to reprint a technical paper or permission to use copyrighted SAE publications in other works, contact the SAE Publications Group.



**GLOBAL MOBILITY DATABASE**

*All SAE papers, standards, and selected books are abstracted and indexed in the Global Mobility Database*

No part of this publication may be reproduced in any form, in an electronic retrieval system or otherwise, without the prior written permission of the publisher.

**ISSN 0148-7191**

**Copyright 2001 Society of Automotive Engineers, Inc.**

Positions and opinions advanced in this paper are those of the author(s) and not necessarily those of SAE. The author is solely responsible for the content of the paper. A process is available by which discussions will be printed with the paper if it is published in SAE Transactions. For permission to publish this paper in full or in part, contact the SAE Publications Group.

Persons wishing to submit papers to be considered for presentation or publication through SAE should send the manuscript or a 300 word abstract of a proposed manuscript to: Secretary, Engineering Meetings Board, SAE.

**Printed in USA**

# Experiment and Numerical Simulation of Unsteady Temperature Fields in Automotive Catalytic Converters

Jian-Xin Wang, Shi-Jin Shual and Ren-Jun Zhuang  
State Key Laboratory of Automotive Safety and Energy, Tsinghua Univ.

Copyright © 2001 Society of Automotive Engineers, Inc.

## ABSTRACT

This paper measured unsteady temperature fields of uncoated-monolith and catalytic monolith under real engine operating conditions using thermocouples. A multi-dimensional flow mathematical model of the turbulence, heat and mass transfer, and chemical reactions in monoliths was established using a computational fluid dynamics (CFD) code and numerically solved in the whole flow field of the catalytic converter. The purpose of this paper is to study unsteady warm-up characteristics of the monoliths and to investigate effects of inlet cone structure on temperature distribution of the catalytic converter. Experimental results show that the warm-up behaviors between uncoated-monolith and catalytic monolith are quite different. Simulation results indicate that the established model can qualitatively predict the warm-up characteristics. Increasing the inlet cone angle can improve the light-off characteristics of the catalysts due to high flow velocity and high temperature in the center of the monoliths.

## INTRODUCTION

New vehicle emission regulations equivalent to Euro I have been implemented in China since Jan. 2000 and Euro II will also be carried out in 2004 early or later. Emission regulations in China should be the same as those developed European countries near 2010 year. According to existed experiences in the world<sup>[1]</sup>, the main emission control technology for gasoline vehicles which can meet Euro II and Euro III is still the three-way catalytic converter (TWC) plus electronic fuel injection (EFI) system. But a match of TWC with EFI and an optimum design of catalytic converter exhaust system should be more careful and refined. The main challenge is how to reduce the hydrocarbon (HC) emitted from vehicles during the cold start. According to vehicle driving cycle tests, approximately 80 percent of HC is emitted in cold start phase due to a low temperature of the exhaust gas and monolith<sup>[2]</sup>. Therefore, how to increase HC conversion efficiency during the cold start is a key factor to satisfy the stringent emission regulations. In this paper, temperature fields of the monoliths were measured and simulated to study temperature

distributions and warm-up characteristics of the catalytic converter.

## MEASUREMENT OF TEMPERATURE IN MONOLITH

### EXPERIMENTAL EQUIPMENT

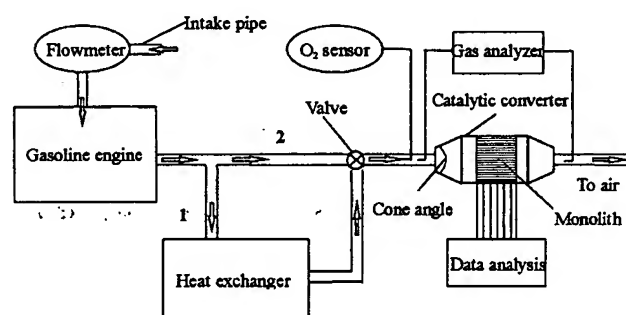


Figure 1. Schematic of test rig

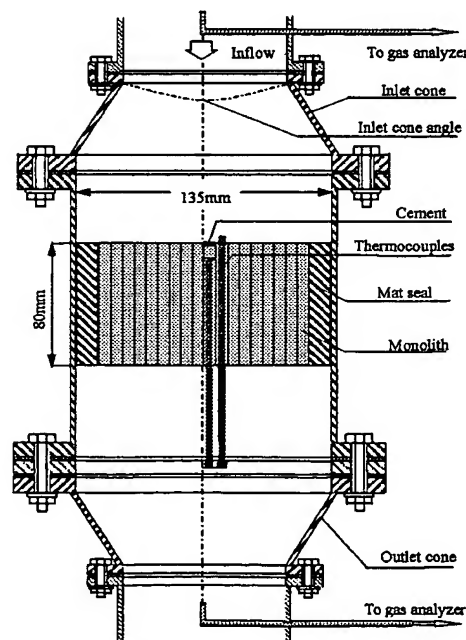


Figure 2. Installation of thermocouples in converter

A schematic of test rig and the installation of thermocouples in the catalytic converter are shown in Figure 1 and Figure 2 respectively. The test engine is BN492 S.I. engine with a single point injection (SPI) system. Three-way catalyst monolith is used as a catalytic monolith. Uncoated-monolith is made of cordierite ( $2\text{MgO} \cdot 2\text{Al}_2\text{O}_3 \cdot 5\text{SiO}_2$ ), with a porosity of 300 cpsi. The NiCr-NiSi thermocouple used in the experiment is 1 mm in diameter. From the rear end of the monoliths, the thermocouples are inserted into the channels at different positions along radial and axial directions (also see Figure 3 below). The inlets of the test channels are sealed by temperature-resisting cement to measure the temperature of the monoliths. Several thermocouples protrude their heads 10 mm out of the channels to measure the inflow gas temperature, as shown in Figure 2. Exhaust gas from the engine has two routine lines (1 and 2 as shown in Figure 1) to enter the catalytic converter, one is to pass through the heat exchanger, and another is to enter the converter directly. The heat exchanger installed in routine 1 is used to cool the hot exhaust gas to a fixed temperature for an initial test temperature, which is greatly lower than the light-off temperature of the catalyst. The control valve turns the exhaust gas from routine 1 to routine 2 when the measurement begins.

#### ARRANGEMENT OF MEASURING POINTS

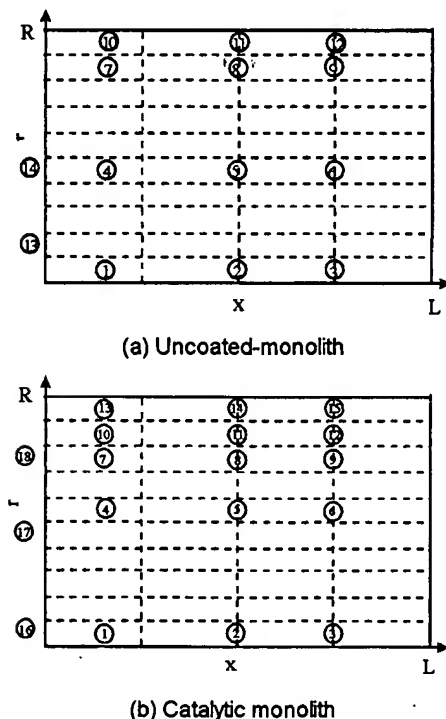


Figure 3. Arrangement of measuring points

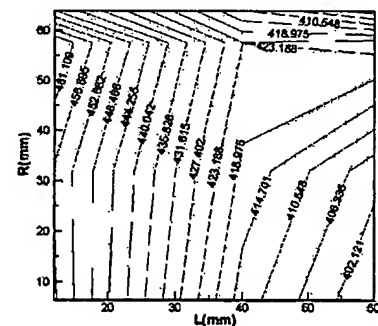
The measuring points of the thermocouples in axisymmetric planes of uncoated-monolith and catalytic monolith are arranged as shown in Figure 3(a) and (b) respectively. The points are mainly distributed in the center and near the edge of the monoliths. Along axial

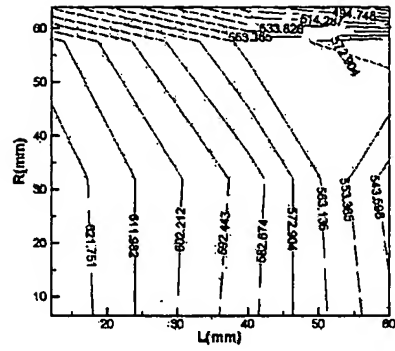
direction, the thermocouples are located at three cross-sections with x coordinates of 0.15L, 0.5L and 0.75L. Along radial direction, they are located at the positions with r coordinates of 0.1R, 0.5R, 0.9R and 1R for uncoated-monolith, and 0.1R, 0.6R, 0.8R and 0.9R for catalytic monolith. In order to obtain the gas temperatures into the monoliths, three points with r coordinates of 0.1R, 0.5R and 0.8R are chosen for uncoated-monolith, and two points with r coordinates of 0.1R and 0.5R for catalytic monolith.

#### TEST RESULTS AND ANALYSIS

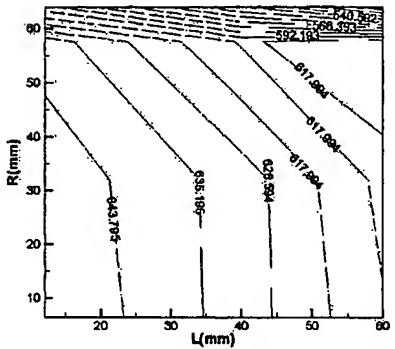
##### Warm-up characteristics of uncoated-monolith

Researches on warm-up characteristics of uncoated-monolith can help us to understand the effect of the monolith itself on light-off performance of the catalyst. The catalytic converter used in this experiment has an inlet cone angle of  $40^\circ$ . The engine running conditions are as follows: engine speed is 2000 r/min; A/F (air/fuel ratio) is controlled near stoichiometric ratio; mass flow in the catalytic converter is 33.3 g/s. Before measuring, the exhaust gas passes through routine 1 pipe (see also Figure 1) and is cooled by the heat exchanger and then goes into the catalytic converter. In this case, the inlet gas temperature is controlled at about  $150^\circ\text{C}$ . When the engine runs steadily, turn the valve rapidly to routine 2 to let the exhaust gas enter the converter directly. At the same time, record the temperature rising process at different time using data sampling and analyzing system.

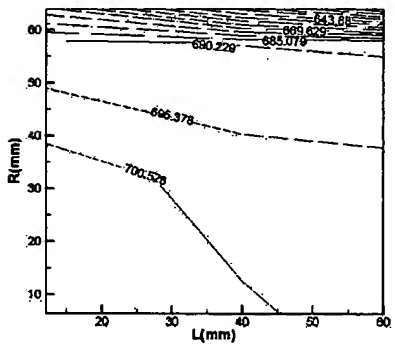




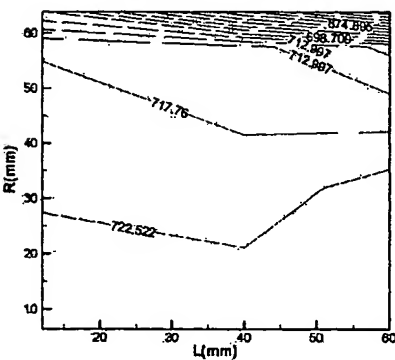
(c) 15 second



(d) 20 second



(e) 60 second



(f) 90 second

Figure 4. Temperature contours in uncoated-monolith at different time

Figure 4(a)~(f) show temperature contour changes in uncoated-monolith. These contours illustrate the distribution and development of the temperature field in the monolith at  $x=0.15L\sim0.75L$  along axial direction and  $r=0.1R\sim1R$  along radial direction. The front center of the monolith has a highest temperature due to a high flow velocity in the center of the monolith<sup>[3]</sup>. As time goes on, the high temperature field expands to the surrounding area and also moves backwards with the heat flux transfer along axial and radial directions. And the temperature gradient decreases gradually and the temperature tends to be more and more uniform. Figure 4(e) and (f) are temperature contours at 60 second and 90 second respectively. From the two figures we can see that the temperature difference between the two moments is not obvious, which indicates that the temperature in uncoated-monolith tends to be stable after 60 second. But the temperature in the edge of the monolith is still lower than that in the center because of the heat exchange with circumference near the edge.

#### Warm-up characteristics of catalytic monolith

For catalytic monolith, not only is there a convective heat transfer between the monolith and the exhaust gas, but also a large amount of heat released from the chemical reactions on the surface of the monolith. Consequently, the unsteady temperature field of catalytic monolith is quite different from uncoated-monolith. Here, all the engine test conditions and measuring process are the same as mentioned above in uncoated-monolith. But catalytic monolith has 15 measuring points more than uncoated-monolith.

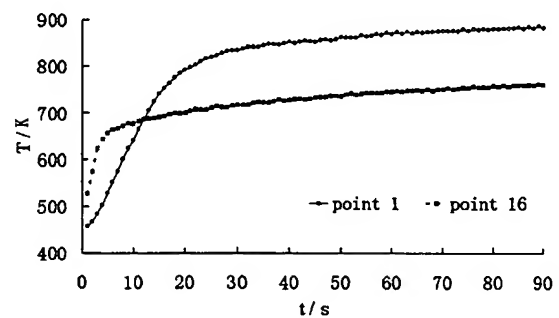


Figure 5. Warm-up behaviors at point 1 and point 16

Figure 5 shows the warm-up behaviors of measuring point 1 and point 16, which gives the temperature of the front center of the monolith and the temperature of the exhaust gas into the monolith respectively as shown in Figure 3. The figure indicates that the temperature of the monolith (point 1) is lower than that of the exhaust gas (point 16) at the beginning of the warm-up. But after about 12 second, the temperature of point 1 begins to exceed the temperature of point 16, which means that the catalyst is activated and the released heat is now heating the monolith.

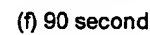
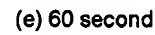
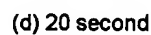
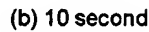
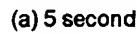


Figure 6(a)-(f) are temperature contours in catalytic monolith at different time. Compared with Figure 4, it is found that the development trend of unsteady temperature fields of catalytic monolith is similar to uncoated-monolith at the beginning (before the catalyst is activated), that is to say, the front center of the monolith has the highest temperature and then the high temperature field expands and moves backwards as time goes on. This is because the monolith is mainly heated by the exhaust gas during this period, and its temperature increases slowly. After the catalyst is activated, the heat from chemical reactions results in a sudden rise of the temperature in the front part. As a result, the development of temperature field in catalytic monolith is quite different from that in uncoated-monolith. From Figure 6(e) and (f) it can be seen that at 60 second the temperature in the rear center of the monolith is close to the front part; but at 90 second the temperature in the rear center is higher than that in the front part. The main reason is that after the catalyst is activated, the monolith temperature in the front part is greatly higher than the exhaust gas. At this time the exhaust gas actually cools the monolith, so not only is the chemical reaction heat brought away by the exhaust gas, but also the growth rate of the temperature in the front part is lowered by the convective heat transfer. However, temperatures of the middle and the rear part are a little low at the beginning, then the hot exhaust gas and released chemical reaction heat from the upstream

accelerate chemical reactions downstream. Therefore, a high temperature field appears in the middle and rear part of the monolith.

The contours also indicate that the temperature gradient on the whole monolith is very small at 5 second, the difference between the highest temperature and the lowest one is about 70 °C. After the catalyst is activated, the difference grows quickly due to the heat from the chemical reactions in the monolith, for example, the difference at 10 second is about 140 °C and at 15 second it is up to about 185 °C; 20 second later, the difference begins to decrease and tends to be constant about 70 °C as time goes on.

## NUMERICAL SIMULATION OF THE CATALYTIC CONVERTERS

In the past people designed the catalytic converter mainly relying on their experiences, which not only wasted a large amount of time but also cost much of money and manpower. With the rapid development of the computer technology and CFD in recent years, people can utilize numerical simulation method to study the catalytic converter performance<sup>[4]</sup>. This paper uses a CFD code STAR-CD to simulate the transient temperature fields of the catalytic converter and investigates the effect of inlet cone structure on temperature distribution and warm-up characteristics in monoliths.

## MODELS OF FLOW, HEAT AND MASS TRANSFER, CHEMICAL REACTIONS IN MONOLITHS

A two-dimensional computational region of the axis-symmetric catalytic converter (also see Figure 2) is divided into a free stream region and a monolith region as shown in Figure 7. The monolith region can also be subdivided into a fluid region and a corresponding solid region. This paper considers the heat and mass transfer, chemical reactions between the gas and the monolith surface, and also the heat conduction in the monolith.



Figure 7. Computational region of the catalytic converter

### Flow governing equation

For the fluid dynamics that occur in the free stream region the Reynolds averaged Navier-Stokes equations are solved, where the standard  $k-\varepsilon$  turbulence model is used to close the equations. In the monolith an equivalent continuum approach<sup>[5]</sup>, which views the monolith as a porous medium through which the unidirectional gas continually passes, is utilized to establish the models.

The gas flow in parallel channels of the monolith can be regarded as a fully developed laminar flow whose governing equation is given by Hagen-Poiseuille equation as follows:

$$\frac{\partial p}{\partial x} = \frac{-32\nu\rho U}{ad^2} \quad (1)$$

where  $U$  is the gas velocity,  $\alpha$  is the monolith porosity,  $d$  is the hydraulic diameter of monolith channels. The gas viscosity  $\nu$  which is a function of gas temperature  $T_g$  is given by<sup>[6]</sup>:

$$\nu = (6.542 \times 10^{-11} T_g^2) + (6.108 \times 10^{-8} T_g) - 0.89 \times 10^{-5} \quad (2)$$

### Heat and mass transfer equations

#### Gas enthalpy conservation equation

$$\frac{\partial(\rho_g h_g)}{\partial t} + \frac{\partial}{\partial x}(\rho_g U h_g) = h a_s (T_s - T_g) \quad (3)$$

where  $\rho_g$  is the gas density;  $h$  is the gas heat transfer coefficient;  $a_s$  is the ratio of monolith surface to monolith volume;  $T_s$  is the monolith temperature and the gas temperature  $T_g$  is obtained by:

$$T_g = h_g / C_{pg} \quad (4)$$

where  $h_g$  is the gas enthalpy and  $C_{pg}$  is the gas specific heat capacity.

#### Chemical species conservation equation

$$\frac{\partial \rho_g c_{gi}}{\partial t} + \frac{\partial}{\partial x}(\rho_g U c_{gi}) = \rho_g K_{mi} a_s (c_{si} - c_{gi}) \quad (5)$$

where  $c_{gi}$  is the mass fraction of species  $i$  in the gas and  $c_{si}$  is the mass fraction of species  $i$  on the surface of the monolith;  $K_{mi}$  is the mass transfer coefficient of species  $i$ . The concentrations of the species on the catalyst surface are governed by expressions of the form:

$$\rho_g K_{mi} a_s (c_{si} - c_{gi}) = \frac{M_i R_i}{10^3} \quad (6)$$

where  $M_i$  is the molecular mass of species  $i$ ;  $R_i$  is the chemical reaction rate of species  $i$ . The term on the left side of equation (6) represents the diffusion process of species to and from the monolith surface. The term on the right side indicates the removal of species by reaction.

#### Monolith heat conduction equation

The equation governing the monolith temperature  $T_s$  behavior is essentially that of heat conduction in the monolith. Considering the orthotropic nature of the heat conduction, the governing equation takes the form:

$$(1-\alpha)c_s \rho_s \frac{\partial T_s}{\partial t} - k_s [(1-\alpha) \frac{\partial^2 T_s}{\partial x^2} + G(\frac{\partial^2 T_s}{\partial y^2} + \frac{\partial^2 T_s}{\partial z^2})] = s_1 + s_2 \quad (7)$$

where  $x$  is the gas flow direction;  $y$  and  $z$  are another two coordinate directions perpendicular to  $x$  direction;

$\rho_s$  is the monolith density;  $c_w$  is the monolith specific heat;  $k_s$  is the monolith thermal conductivity;  $G$  is the monolith anisotropic conductivity factor in  $y$  and  $z$  directions. The two source items  $s_1$  and  $s_2$ , are given by:

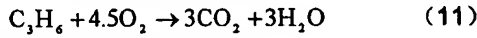
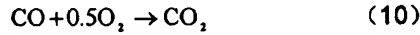
$$s_1 = ha_s(T_s - T_r) \quad (8)$$

$$s_2 = \sum R_i \Delta H_i \quad (9)$$

where  $s_1$  is the heat transfer between the monolith and the gas;  $s_2$  is the heat released from chemical reactions;  $\Delta H_i$  is the reaction heat of species  $i$ .

### Chemical reaction equations

The chemical reactions of the catalysts on the monolith surface are very complex. This paper only considers the oxidation reactions of CO and C<sub>3</sub>H<sub>6</sub><sup>[4]</sup> occurred on the surface as a preliminary investigation. Propylene (C<sub>3</sub>H<sub>6</sub>) is assumed to be a representative of "fast oxidizing hydrocarbons". The simplified chemical reactions can be expressed by:



and the reaction rates are given by:

$$R_{\text{CO}} = \frac{k_1 c_{\text{CO}} c_{\text{O}_2}}{D(T_s, c)} \quad (12)$$

$$R_{\text{C}_3\text{H}_6} = \frac{k_2 c_{\text{C}_3\text{H}_6} c_{\text{O}_2}}{D(T_s, c)} \quad (13)$$

where

$$D(T_s, c) = T_s (1 + K_1 c_{\text{CO}} + K_2 c_{\text{C}_3\text{H}_6})^2 (1 + K_3 c_{\text{CO}}^2 c_{\text{C}_3\text{H}_6}^2) (1 + K_4 c_{\text{NO}}^{0.7}) \quad (14)$$

$$k_1 = 6.699 \times 10^9 \exp(-12556/T_s) \quad (15)$$

$$k_2 = 1.392 \times 10^{11} \exp(-14556/T_s) \quad (16)$$

$$K_1 = 65.5 \times \exp(961/T_s) \quad (17)$$

$$K_2 = 2.08 \times 10^3 \exp(361/T_s) \quad (18)$$

$$K_3 = 3.98 \times \exp(11611/T_s) \quad (19)$$

$$K_4 = 4.79 \times 10^3 \exp(-3733/T_s) \quad (20)$$

From the stoichiometry the reaction rate for oxygen must satisfy the following relation:

$$R_{\text{O}_2} = 0.5R_{\text{CO}} + 4.5R_{\text{C}_3\text{H}_6} \quad (21)$$

### SOLUTION CONDITIONS

The PISO algorithm is used to solve the above governing equations for transient flows. Subroutines for heat and mass transfer and chemical reactions on the monolith surface are programmed by authors and solved coupling with the flow governing equations in free stream region (see also Figure 7). The detailed solution process can be referred to the literature [7].

### Boundary conditions

#### Inlet boundary

The inlet velocity at the entrance of the catalytic converter is assumed to be uniform and flows along the

symmetrical axis of the converter. Here the inlet velocity  $V_{in}$  is 21.2 m/s calculated from the above measurement of the mass flow, and the density  $\rho_{in}$  is assumed to be 1.0 kg/m<sup>3</sup>. The inlet mass fractions of the species are supposed as follows:  $c_{\text{CO}_2} = 0.0048$  kg/kg,  $c_{\text{O}_2} = 0.022$  kg/kg,  $c_{\text{C}_3\text{H}_6} = 0.00065$  kg/kg. The turbulent kinetic energy  $\kappa$  is assumed to be 0.02 m<sup>2</sup>/s<sup>2</sup> and its dissipation rate  $\varepsilon = 0.01$  m<sup>2</sup>/s<sup>3</sup>. The inlet temperature changes as shown in Figure 8.

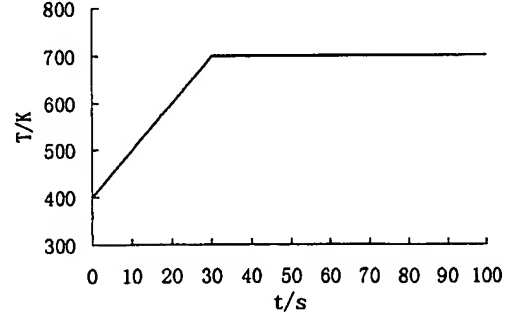


Figure 8. Inlet temperature vs. time

#### Outlet boundary

The outlet boundary condition is treated as a fully developed flow, namely the gradients of all variables (except pressure) are zero. The outlet mass flux must satisfy the mass conservation.

#### Wall boundary

Wall boundary conditions are no-slip velocity boundary and adiabatic temperature boundary. The inlet and outlet ends of the monolith are also treated as an adiabatic temperature boundary.

### Initial conditions

In the whole region of the catalytic converter, the initial velocity and concentrations of O<sub>2</sub>, CO, C<sub>3</sub>H<sub>6</sub> are set to be zero and the temperature is assumed to be 400 K.

## SIMULATION RESULTS AND ANALYSIS

### Warm-up characteristics of the catalytic converter

Figure 9(a)~(h) show the temperature contours in the catalytic converter with a 40° cone angle at different time. The upper part of the figures illustrates the distribution of the monolith temperature  $T_s$  and the down part is the distribution of the gas temperature  $T_g$ . From the figures we can see that the inlet temperature of the monolith is only 500 K at 10 second and the catalyst is not activated. At this time the temperature behind the monolith maintains the initial temperature of 400 K. At 20 second the inlet temperature of the monolith rises to 600 K and the catalyst is lighted off. Then the temperature in the front part of the monolith increases quickly and the gas temperature behind the monolith also begins to rise



gradually. At 30 second the inlet temperature goes up to 700 K and the highest temperature in the front part of the monolith reaches 734 K due to the heat released from chemical reactions, which is higher than the inlet temperature at the moment. From 30 second to 40 second, the rising rate of the temperature in the monolith closes to the highest about 5.7 K/s. After 40 second the temperature changing trend becomes slow. At 60 second the gas temperature behind the monolith is close to the inlet temperature. At 80 second, the temperature behind the monolith greatly exceeds the inlet temperature and the highest temperature reaches 755 K. At the same time the temperature in the whole region of the catalytic converter gradually tends to be stable. At 100 second all of the temperatures are nearly uniform and stable. The highest temperature is up to 813 K. From the above analysis of the warm-up behavior in the catalytic converter, it can be concluded that the monolith explores a series of heating processes by inlet gas flow and chemical reactions. The temperature difference in the monolith changes from a small value at the beginning to a large one and again to a small one at the end. The computed warm-up characteristics of the monolith have a qualitative agreement with the test results above. This means that the established model in this paper can essentially display the features of the flow, heat and mass transfer and chemical reactions occurred in catalytic converters.

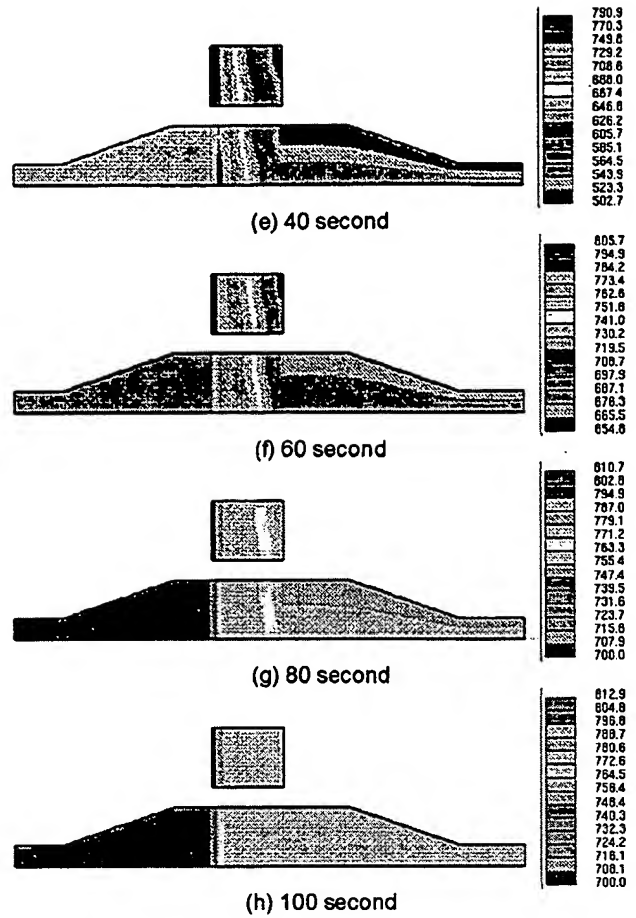
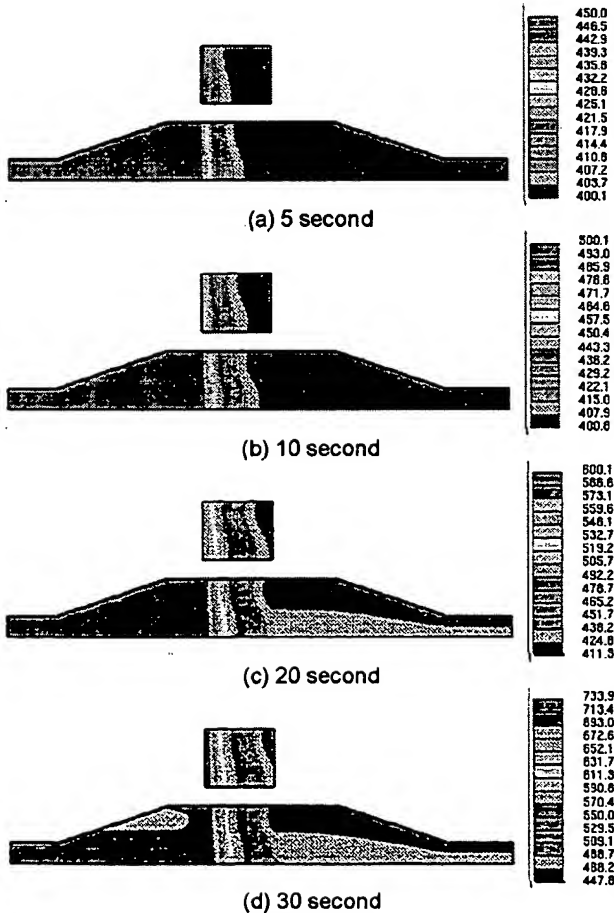
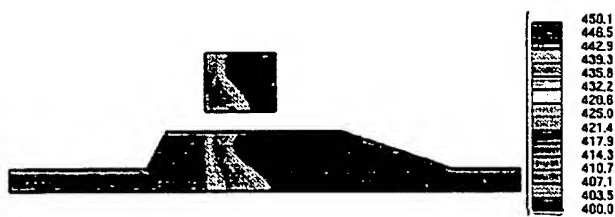


Figure 9. Temperature contours of 40° catalytic converter at different time (K)

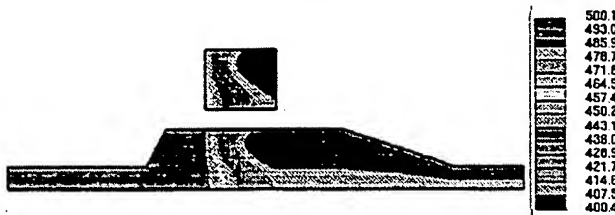
#### Effect of inlet cone structure on warm-up characteristics

In order to investigate the effect of the inlet cone structure on the temperature distribution, the flow including heat and mass transfer and chemical reactions in the catalytic converter with a 120° cone angle is also simulated. Compared with the 40° catalytic converter, the 120° catalytic converter has the same computational conditions except for a different cone angle.

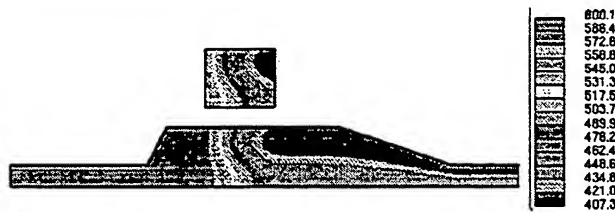
Figure 10(a)~(h) show the temperature contours in the catalytic converter with a 120° cone angle at different time. From the comparison between Figure 9 and Figure 10 it is found that there are some differences existed in the temperature distribution and warm-up behavior between two converters although they have a similar temperature change trend. For the 120° catalytic converter the catalyst is not lighted off at 10 second. In this case two catalytic converters have no obvious differences for the temperature distribution along axial direction, but the 40° catalytic converter has a more uniform temperature distribution along radial direction.



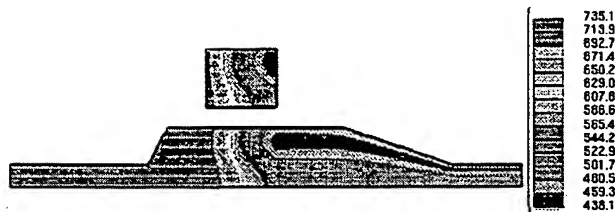
(a) 5 second



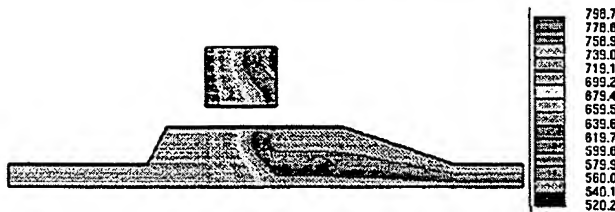
(b) 10 second



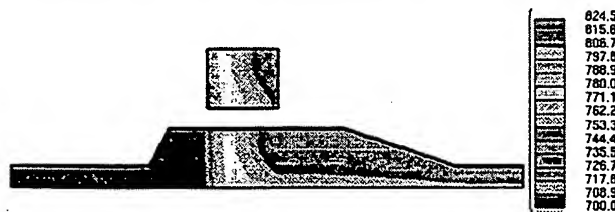
(c) 20 second



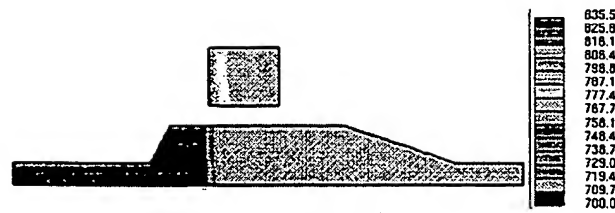
(d) 30 second



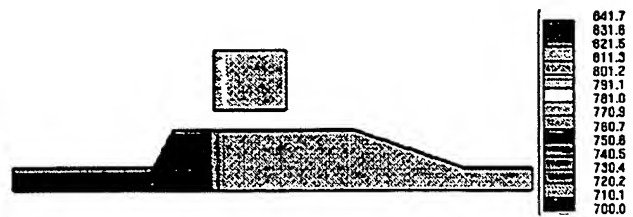
(e) 40 second



(f) 60 second



(g) 80 second



(h) 100 second

Figure 10. Temperature contours of 120° catalytic converter at different time (K)

Figure 11 shows the comparison of the temperature distribution along radial direction in the middle sections of the monoliths at 10 second. From the figure it can be seen that for the 120° catalytic converter the temperature difference between the center and the edge in the monolith is about 30 K, but for the 40° catalytic converter it is less than 10 K. This temperature distribution is consistent with the velocity distribution in the same location at the same time, as shown in Figure 12, which means that the gas velocity has a significant influence on the temperature distribution in catalytic converters.

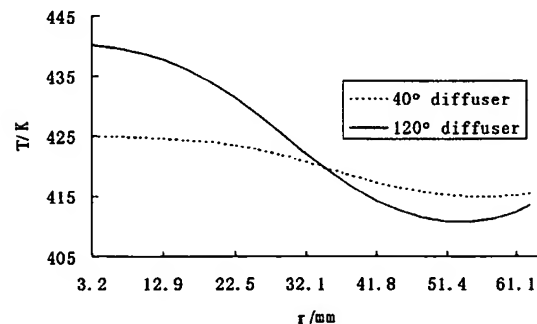


Figure 11. Temperature distribution in middle cross section

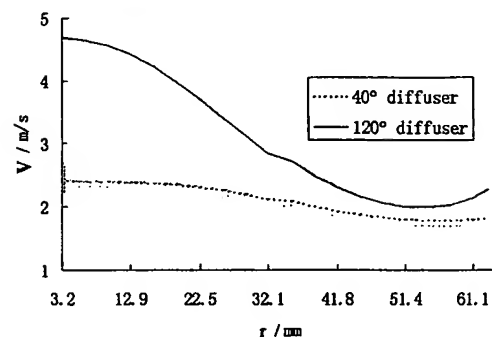


Figure 12. Axial velocity distribution in middle cross section

Figure 13 and Figure 14 show the warm-up behaviors at the center and at the edge in the middle section of the monoliths respectively. From these figures we can clearly see that the temperature of 120° converter exceeds the temperature of 40° converter as time goes on, and the largest temperature difference is more than 50 K at about 40 second. However, as the temperature tends to be stable, the difference becomes smaller and

smaller. In addition, the difference is larger at the center than at the edge. This is because the flow velocity at the center of 120° converter is higher than that of the 40° converter (also see Figure 12) and the inlet temperature can quickly conduct into the monolith, which results in a rapid light-off of the catalysts. Moreover, the heat released from chemical reactions accelerates the warm-up of the monolith.

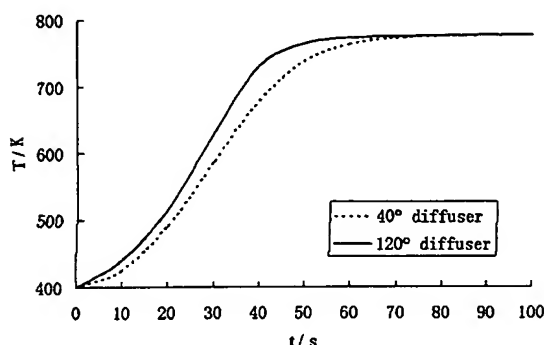


Figure 13. Warm-up characteristics at the center

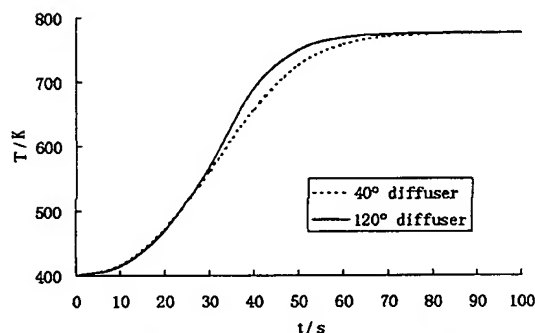


Figure 14. Warm-up characteristics at the edge

## CONCLUSION

From the experiment and numerical simulation of the temperature fields of the catalytic converters, the conclusions can be drawn as follows:

1. Heat convective transfer between the exhaust gas and the monolith, heat conduction in the monolith, heat from chemical reactions, and flow velocity distribution are all main factors affecting the temperature distribution and warm-up characteristics.
2. For uncoated-monolith, high temperature always appears in the front center of the monolith. As time

goes on, the high temperature region expands and moves backwards.

3. For catalytic monolith, when the catalyst is not activated, the temperature distribution and warm-up characteristics of the monolith are similar to uncoated monolith. However, after the catalyst is activated, the high temperature appears in the rear center part of the monolith.
4. A multi-dimensional flow including heat and mass transfer, chemical reactions is numerically simulated. Although the model contains many simplifications and assumptions it has been demonstrated that it can predict the warm-up behavior of the catalytic converter and the effect of the inlet cone structure on the warm-up behavior.
5. Simulation results show that the 120° catalytic converter has a better light-off performance than the 40° catalytic converter, especially in the center of the monolith.
6. Further study includes quantitative validation of the model, the modeling of more than two reacting species, external heat loss and the thermal inertia effects of the catalyst matting and can.

## ACKNOWLEDGMENTS

This research is supported by Beijing Science and Technology Committee, Grant No. 954062400.

## REFERENCES

1. Mondt, J.R.. Cleaner Cars: The History and Technology of Emission Control Since the 1960s. Society of Automotive Engineers Inc., Warrendale, Pa. 2000
2. Glander, G. and Zidat, S.. Modeling Electrically Heated Converters. Automotive Engineering International. 1998, No.2, pp: 76-78
3. Shuai, S.J., Wang, J.X., Zhuang, R.J., et al. Study on Flow Characteristics of Automotive Catalytic Converters with Various Configurations. SAE Paper 2000-01-0208
4. Chen, D.K.S., Bissett, E.J., Oh, S.H., et al. A Three-dimensional Model for the Analysis of Transient Thermal and Conversion Characteristics of Monolithic Catalytic Converters. SAE Paper 880282
5. Zygorakis K. Transient operation of monolith catalytic converter: A two-dimensional reactor model and the effects of radially nonuniform flow distributions. Chem. Eng. Sci., Vol.44, 1989, pp 2075-2086
6. Clarkson R.J., Benjamin S.F., Jasper T.S., and Girgis N.S.. An integrated computational model for the optimization of monolith catalytic converters. SAE Paper 931071
7. Shuai, S.J.. Numerical Simulation of Flow Fields and Temperature Fields in Automotive Catalytic Converter and Its Optimum Structure Design. Tsinghua University, Postdoctoral Research Report, 2000